Desalination and Water Treatment
www.deswater.com

doi: 10.5004/dwt.2017.20921

78 (2017) 41–48
June

New ceramic microfiltration membrane from Tunisian natural sand: application for tangential wastewater treatment

Hajer Aloulou[a], Hazem Bouhamed[b], Raja Ben Amar[a], Sabeur Khemakhem[a,*]

[a]*Laboratoire Sciences des Matériaux et Environnement, Faculté des Sciences de Sfax, Université de Sfax, Route de Soukra Km 4, 3038 Sfax, Tunisia, Tel. +216 74241403; Fax: +216 74246347; email: khemakhem_sabeur@yahoo.fr (S. Khemakhem), hajer.aloulou89@yahoo.fr (H. Aloulou), benamar.raja@yahoo.com (R.B. Amar)*
[b]*Laboratoire de Chimie Industrielle (LCI), Ecole Nationale d'Ingénieurs de Sfax (ENIS), BP 1173, 3038 Sfax, Tunisia, email: hazem.bouhamed@gmail.com*

Received 8 January 2017; Accepted 6 May 2017

ABSTRACT

New ceramic supports from low-cost natural Tunisian sand have been prepared and characterized. Plastic paste has been prepared from sand powder (average particle size ≈ 100 μm) mixed with organic additives and water. The obtained paste has been extruded to porous tubular supports. After firing at 1,250°C/3 h, the support has shown a porosity of 44.72% and an average pore diameter of 10.36 μm. SEM analysis has shown smooth and cracks-free surface of the tubular supports. The tubes have displayed good chemical and mechanical properties. The water permeability of the sand support sintered at 1,250°C/3 h has been 3,611 L/h m^2 bar. Microfiltration layer has been also prepared from the same natural sand powder (average particle size <50 μm) by the slip casting method using a mixture of powder sand, water and polyvinyl alcohol solution. The water permeability of the microfiltration membrane sintered at 1,100°C/3 h has been 1,228 L/h m^2 bar. The obtained microfiltration membrane has been tested for the treatment of cuttlefish effluent. The membrane has displayed better separation performance in terms of chemical oxygen demand and turbidity removal.

Keywords: Ceramic support; Tunisian sand; Extrusion; Microfiltration membrane

1. Introduction

Membrane technologies have been widely utilized in different fields, such as chemistry, biotechnology, food and lately wastewater treatment [1]. According to the literature, there are three generations of membranes [2]: organic membranes with cellulose acetate, organic membranes with polymers of synthesis and recently mineral membranes in carbon and aluminum oxide. Many efforts to achieve efficient and economical membranes for different uses have been resulted in a selection of new materials, an improvement in ceramic membrane preparation techniques and an increase in the range of applications [3,4]. The use of inorganic membranes has many benefits such as chemical stability, high pressure, thermal resistance, long lifetime and catalytic properties from their intrinsic nature [5–7]. Conventionally, alumina, zirconia, titania and silica have been classed as the main materials of commercialized ceramic membranes [8]. Unfortunately, these membranes are too expensive from a technico-economic point of view. Conventionally, alumina (α-Al_2O_3) has been considered as the main body material for commercialized ceramic membrane supports. However, both expensive raw materials and high cost of sintering, limit alumina applications in many industrial fields. For economic consideration, an exceptional agreement of research has been dedicated to the progress of a new type of supports made from low-cost natural materials. From the literature, Saffaj et al. [9] and Loukili et al. [10] have used the natural Moroccan clay to produce membrane supports for ultrafiltration and microfiltration applications. On the other hand, granitic and clay sands have been utilized by Rakib et al. [11]

* Corresponding author.

to elaborate membrane support for tangential ultra-filtration and microfiltration membranes. Similarly, Bouzerara et al. [12] have prepared membrane supports with Algerian clay. Sarkar et al. [13] have developed membrane supports based on Indian clay. Chen et al. [14] have prepared membrane supports by Chinese clay. There are researchers who have developed membrane supports with cordierite as Dong et al. [15] and Liu et al. [16].

Furthermore, the development of mineral-based microfiltration membranes can lead to a critical new technological revolution that would add an important economic value to natural minerals present throughout the world. In fact, Dong et al. [17] have fabricated low-cost microfiltration membrane using natural zeolite mineral as the starting material. On the other hand, Ivanets et al. [18] have successfully prepared microfiltration membrane using natural quartz sand from Mongolia. Suresh et al. [19] have treated oil–water emulsion using fly ash-based microfiltration membrane. Also, efficient clay membranes have been successfully elaborated by Belibi et al. [20] and Saffaj et al. [21].

Recently, our research team has developed low-cost ceramic membrane supports based on natural materials, such as clay [22], phosphate [23], fly ash obtained from coal fired power station [24], apatite [25] and carbon [26]. These researchers have successfully elaborated new tubular membranes based on their mineral materials [26–30]. This has appeared as a competent solution to treat wastewater.

The present work describes the elaboration of macro-porous support and micro active layer based on Tunisian natural sand. This raw material has been dictated by its beneficial properties and natural abundance. The efficiency of this microfiltration membrane has been evaluated through the application to the treatment of Tunisian cuttlefish effluents.

2. Materials and methods

2.1. Preparation of the powder

The size of the raw sand particles does not achieve the optimum mechanical resistance of the membrane support. Therefore, we have crushed each 50 g of powder for 20 min with the assistance of a mortar crusher (Retsch, France), then we have calibrated with a sieve of 100 μm.

2.2. Characterization of the sand powder

The sand powder comes from Oudhref (Tunisian town located 20 km north of Gabes). The chemical composition of the sand powder has been determined by X-ray fluorescence for metals. Linear shrinkage has been determined by dilatometry (Setaram TMA-92 dilatometer) with a heating rate of 10°C min^{-1}, in the temperature range from the ambient (25°C) to 1,300°C. Thermo-gravimetric analysis (TGA) and differential thermal analysis (DTA) of the sand powder have been carried out at temperature range between 25°C and 1,300°C with a rate of 10°C min^{-1} under static atmospheric conditions (Thermal Analyst Netzsch STA 409 C/CD, Germany). Pore size and porosity of the samples have been measured by mercury porosimetry (mercury porosimeter Pascal 440) at high pressure (400 MPa).

2.3. Elaboration of porous support

The elaboration of the tubular macro-support requires three steps:

- preparation of a plastic paste;
- extrusion of the paste; and
- consolidation by sintering.

The procedure of the ceramic support preparation is described in Fig. 1. The preparation of inorganic paste demands a specific aging and also the use of organic additives to allow the powder dispersion and the adjustment of the paste rheological behavior. The major advantage of the organic additives is that they are removed by combustion during the sintering. The optimized composition of the paste includes the following:

- sand powder: 84 wt%,
- methocel: binder (The Dow Chemical Company , France): 4 wt%,
- amijel: plasticizer (Cplus 12076, Cerestar): 4 wt%, and
- starch: porosity agent (RG 03408, Cerestar): 8 wt%.

The plastic paste has been prepared by mixing the powders in a specific mixer to obtain the best homogeneity of the mineral and organic parts. After dry mixing, a volume of 55 mL of water per 200 g of powders has been added progressively. The obtaining of a "block" has indicated the end of this step. For aging, the ceramic paste has been kept in a closed plastic bag for 24 h under high humidity environment to avoid

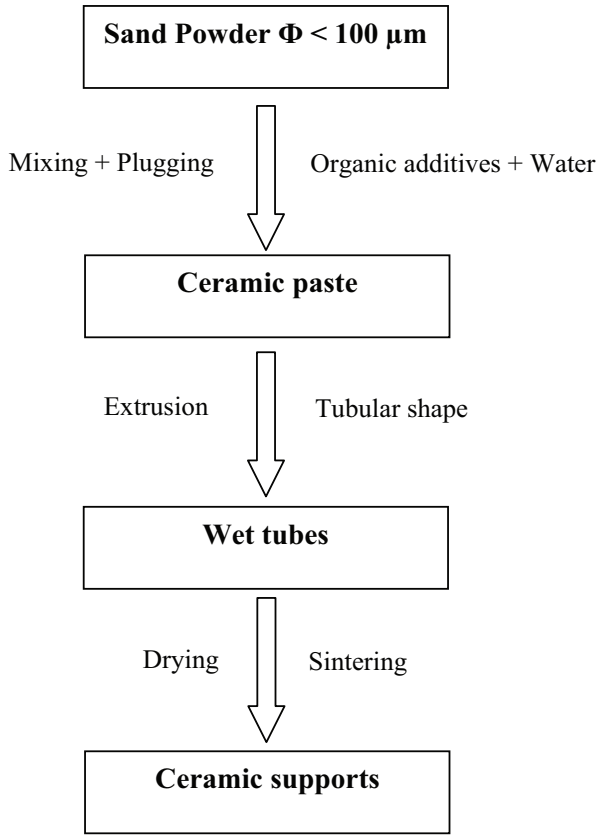

Fig. 1. Main steps of the ceramic support preparation.

premature drying and ensure homogeneous distribution of moisture and organic additives. Shaping has been performed by extrusion with a screw speed of 0.02 m min^{-1}. After that, the wet support has been set on rollers to have a homogenous drying at ambient temperature. Finally, the sintering has been approved out in a programmable furnace at different final temperatures. The adapted firing treatment has been created from the thermal analysis data. Two stages have been defined, the first for the elimination of organic additives at 300°C/2 h and the second for the sintering at different temperatures during 3 h. The temperature–time schedule depends mainly on the porosity, the quality of the surface and the mechanical properties of the final support. The obtained tubular supports have 150 mm of length, 6 mm of internal diameter and 9 mm of external diameter.

2.4. Preparation of the sand microfiltration layer

The same natural powder has been used for the microfiltration layer preparation. The raw sand has been crushed for 15 h with a planetary ball mill Retsch PM 100 at 400 rpm. Then, gravitational sedimentation classification has been performed. The particles of the suspension (12.5 wt% powder loading) have been left to sedimentation for 3 min. After that, the powders in the upper suspension have been collected to sediment for 24 h. Finally, the powder has been dried to obtain ultra-fine sand.

A deflocculated slip has been prepared by mixing 8% (w/w) of the obtained powder, 62% (w/w) of water and 30% (w/w) of polyvinyl alcohol (12% w/w aqueous solution). The deposition of the slip on the porous support has been performed by layer-by-layer process in three steps. For the first coating, the tube has been filled by the slip and emptied immediately. After drying at room temperature for 15 min, the second coating has been done with a deposition time of 1 min. After drying at room temperature for 30 min, the third coating has been realized with an optimal contact time of 10 min. After drying at room temperature for 24 h, the microfiltration layer has been sintered at 1,100°C/3 h after debonding at 250°C/2 h.

2.5. Permeability test

Permeability tests have been performed using a home-made pilot plant [27] at ambient temperature and transmembrane pressure (TMP) ranging between 0 and 1 bar. The flow rate has been fixed at 1.76 m s^{-1}. Before the tests, the support or the membrane has been conditioned by immersion in pure distilled water for a minimum of 24 h. The working pressure has been obtained using a nitrogen gas source. The permeability of the support has been calculated from the fluxes measured after stabilization for all working pressure. The support permeability (L_p) can be determined using the variation of the distilled water flux (J_w) with the TMP (ΔP) following the Darcy's law:

$$J_w = L_p.\Delta P \text{ with } \Delta P = \left(\frac{P_{\text{inlet}} + P_{\text{outlet}}}{2} - P_f \right)$$

P_{inlet} = inlet pressure; P_{outlet} = outlet pressure; P_f = filtrate pressure

3. Results and discussion

3.1. Characterization of the sand powder

3.1.1. Chemical composition

The chemical composition (weight percent) of the sand powder is shown in Table 1. The major chemical component is silica (SiO_2: 95.05%). The other oxides are present in very low amounts (Al_2O_3, $CaCO_3$ and CaO).

3.1.2. Dilatometry analysis

Dilatometry analysis has been carried out on the sand support used in this study to evaluate its extent of shrinkage in the temperature range from 25°C to 1,300°C (Fig. 2). During the heating process, a significant dilation has been observed due to the α-β quartz transition around 573°C. Beyond 620°C, a contraction phenomenon has been occurred until 1,300°C. At 815°C, the speed behavior has changed because of the crystallization of the β-quartz. The sintering process has began at about 1,040°C. The maximum densification speed, corresponding to the inflexion point of the dilatometric curve, has occurred at about 1,140°C. In the temperature range from 1,040°C to 1,300°C, the linear shrinkage has been about 2%. During the cooling step from 620°C to 550°C, dilatometric curve has shown an expansion

Table 1
Chemical composition (wt%) of the sand powder

SiO_2	95.09
Al_2O_3	3.59
$CaCO_3$	2.40
CaO	1.52
Fe_2O_3	0.83
K_2O	0.72
MgO	0.33
Na_2O	0.31
SO_3	0.21
TiO_2	0.03
ZnO	0.01

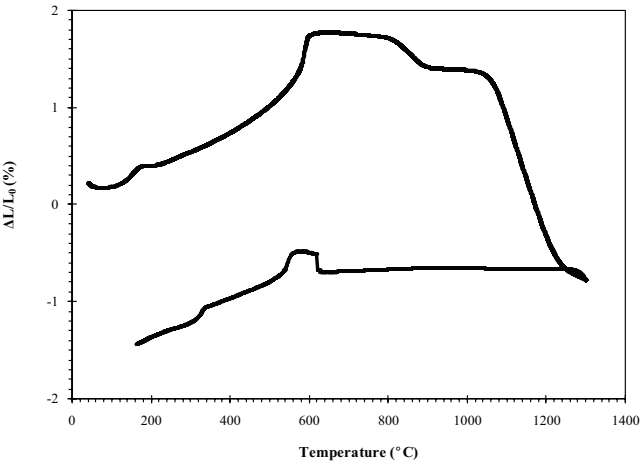

Fig. 2. Dilatometric analysis of the sand powder.

in volume, which is relative to the inverse allotropic transformation from β-quartz to α-quartz.

3.1.3. Thermal analysis

Fig. 3 shows the DTA–TGA curves of the raw sand powder from the ambient temperature (25°C) to 1,300°C. The DTA curve has shown four main endothermic peaks. The two endothermic peaks appeared at 150°C and 250°C correspond to the dehydration of the material. This dehydration is accompanied by a weight loss of 0.6%. The third peak around 570°C characterizes the allotropic transformation of the quartz from α to β, as shown by dilatometric analysis. The last small peak at about 660°C could be attributed to the crystallization of the β-quartz. During the thermal cycle between 25°C and 1,300°C, the total weight loss has not exceeded 2.75%.

3.2. Characterization of the support

The extruded tubes have been sintered at three different temperatures: 1,230°C, 1,250°C and 1,270°C. The choice of these narrow sintering temperatures has been based on the results of porosimetry analysis, SEM study and mechanical tests of supports sintered at different temperatures.

3.2.1. Scanning electron microscopy analysis

The evolutions of densification and surface quality of the support sintered at different temperatures have been examined by scanning electron microscopy (SEM). SEM micrographs of the internal surface of tubular support sintered at 1,230°C, 1,250°C and 1,270°C are shown in Figs. 4(a)–(c), respectively. The formation of grain boundaries has been achieved within this narrow temperature range. The best sintering temperature has been obtained by comparing the texture of patterns sintered at different temperatures. At 1,250°C, the support surface has been homogeneous and has not presented any cracks. A smooth inner surface has been also observed, allowing the effective deposit of an active fine layer membrane. The pore size of the support depends on the sintering temperature. The values estimated from SEM images are 9.50, 10.50 and 11.50 for 1,230°C, 1,250°C and 1,270°C, respectively.

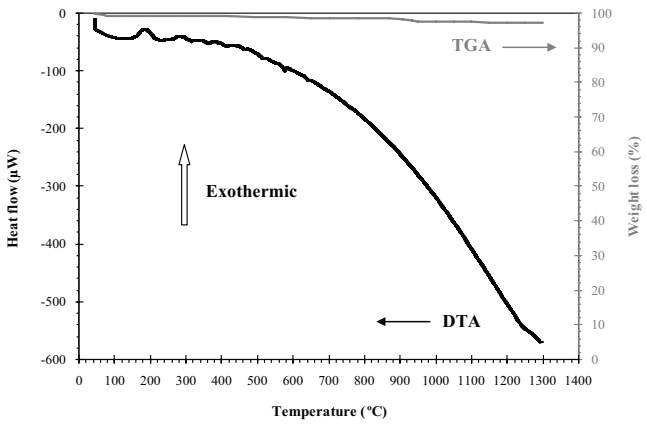

Fig. 3. DTA–TGA curves of the sand powder.

3.2.2. Porosimetry analysis

Pore size and porosity of the support have been measured by mercury porosimetry. The pore size distribution of the sand support sintered at 1,250°C is shown in Fig. 5. Pore size measurements have confirmed the dependence of the pore diameter on the sintering temperature. In fact, the values estimated from mercury porosimetry are 9.25, 10.36 and 11.25 µm for 1,230°C, 1,250°C and 1,270°C, respectively. The pore size values of the sand support estimated from SEM images and mercury porosimetry are shown in Table 2. It is clear that higher the sintering temperature larger the

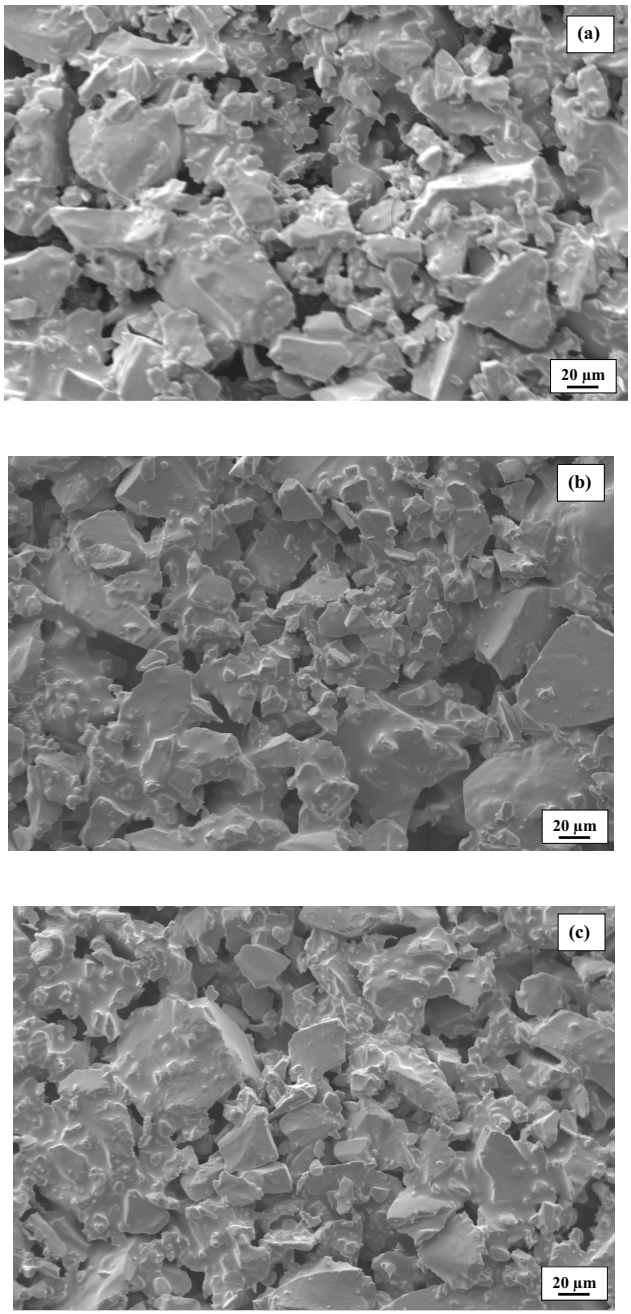

Fig. 4. SEM micrographs of the internal surface of tubular support sintered at 1,230°C (a), 1,250°C (b) and 1,270°C (c).

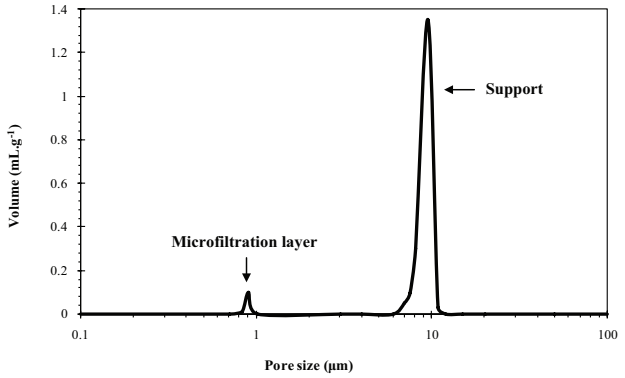

Fig. 5. Pore size distribution of the sand support sintered at 1,250°C and the microfiltration layer sintered at 1,100°C.

Table 2
Pore size of the support and the microfiltration membrane

Sintering temperature (°C)	1,230	1,250	1,270
Pore size of the support (μm)[a]	9.50	10.50	11.50
Pore size of the support (μm)[b]	9.25	10.36	11.25
Pore size of the microfiltration membrane sintered at 1,100°C (μm)[a]	1.0		
Pore size of the microfiltration membrane sintered at 1,100°C (μm)[b]	0.9		

[a]Estimated from SEM images.
[b]Measured by mercury porosimetry.

pore diameter of the support. This result is in agreement with other works [22]. The support sintered at 1,250°C/3 h has reached a mean pore diameter of 10.36 μm and an open porosity of 44.72%, which represent good support properties for microfiltration applications, compared with other mineral supports [9,12,20–23].

3.2.3. Mechanical resistance

Porosity measurements remain not sufficient to optimize the sintering temperature of the ceramic support. It is then necessary to lead a mechanical study according to the sintering temperature. The mechanical resistance tests have been carried out by the three points bending method (Lloyd Instrument, France) to control the resistance of the support tube fired at different temperatures. The dimensions (length/width/thickness) of the samples have been 45mm/12mm/2mm and the distance separating the two points has been 30 mm. Fig. 6 shows the variation of flexural strength vs. sintering temperature of the sand support using three point flexural tests. The increase of the sintering temperature has been accompanied by a densification phenomenon and consequently an increase in the flexural strength (from 13.33 MPa at 1,230°C to 18.56 MPa at 1,270°C). The material sintered at 1,250°C has reached a flexural strength of 15.14 MPa, which represents a good support mechanical resistance, compared with clay or phosphate tubular supports [20–23].

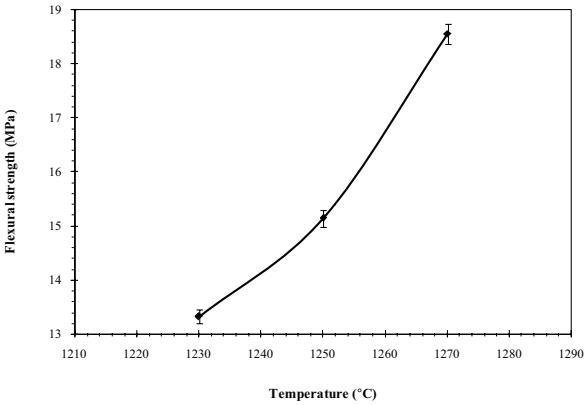

Fig. 6. Flexural strength vs. sintering temperature of the sand support using three point flexural test.

3.2.4. Chemical resistance

For the chemical resistance analysis, we have used HCl 0.2 M and NaOH 0.5 M at the ambient temperature (25°C). The results reported in Figs. 7(a)–(c), show that the sand support sintered at 1,230°C, 1,250°C or 1,270°C presents a chemical resistance towards the acid (HCl 0.2 M) and basic solutions (NaOH 0.5 M). In fact, the weight loss has been negligible when a sample has been placed during 72 h into a soda aqueous solution and has not exceeded 0.2% when it has been placed to a chloride acid aqueous solution in the same conditions in terms of time and temperature. After chemical resistance tests, no phenomenon has been observed in terms of color change, degradation and aging.

3.2.5. Determination of water permeability

The tests have been realized on the support sintered at 1,250°C/3h with a TMP between 0 and 1 bar at room temperature. The corresponding membrane area has been 2.02×10^{-3} m^2. Fig. 8 shows the variation of water flux permeability vs. working pressure of sand support sintered at 1,250°C/3 h and sand membrane sintered at 1,100°C/3 h. It can be noted that the increase of the applied pressure causes a linear increase of the water flux. The support permeability (L_p) has been equal to 3,611 L/h m^2 bar.

3.3. Characterization of the microfiltration layer

3.3.1. Scanning electron microscopy analysis

The morphology and the surface quality of the microfiltration layer sintered at 1,100°C/3 h have been characterized by SEM. SEM micrographs of the surface and the cross section of the microfiltration membrane sintered at 1,100°C/3 h are shown in Figs. 9(a) and (b), respectively. It is clear that there are no cracks and the adhesion between the support and the microlayer is very good. This result confirms the good conditions of filtration layer deposition during the slip casting process. The layer thickness is about 20 μm which is a suitable value for microfiltration layer (Fig. 9(b)). The pore size of the microfiltration membrane sintered at 1,100°C/3 h, estimated from SEM images, has been 1 μm, which is very close to the value measured by mercury porosimetry (0.9 μm), as shown in Fig. 5.

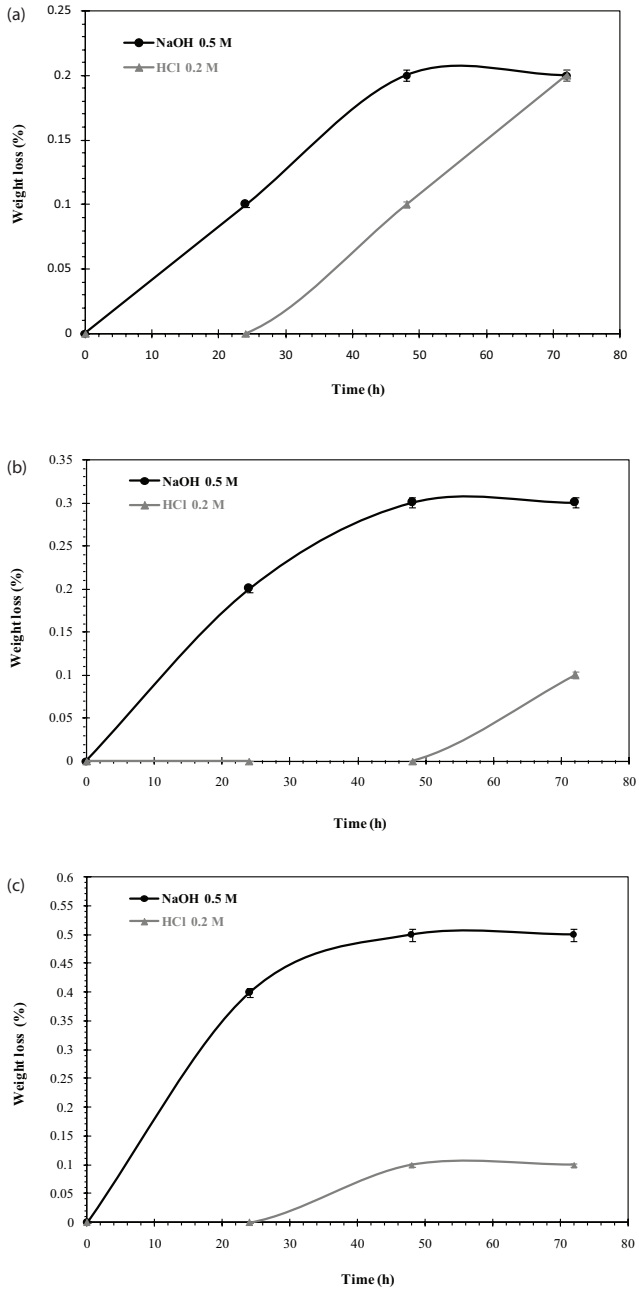

Fig. 7. Weight loss vs. time of support sintered at 1,230°C (a), 1,250°C (b) and 1,270°C (c) in HCl 0.2 M and NaOH 0.5 M.

3.3.2. Determination of microfiltration membrane permeability

Cross-flow microfiltration tests have been realized at room temperature and TMP range between 0 and 1 bar. Before the tests, the microfiltration layer has been immersed in pure distilled water for at least 24 h. It can be noted from Fig. 8 that the increase of the applied pressure causes a linear increase of the water flux. The same evolution has been observed for both support and membrane. The water permeability of the membrane has been 1,228 L/h m^2 bar.

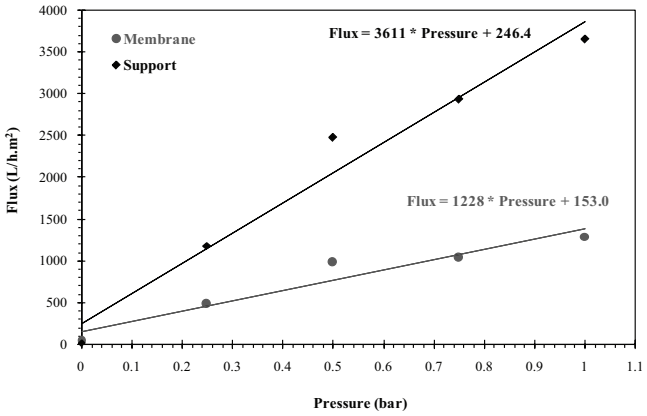

Fig. 8. Water flux permeability vs. working pressure of sand support sintered at 1,250°C and sand membrane sintered at 1,100°C.

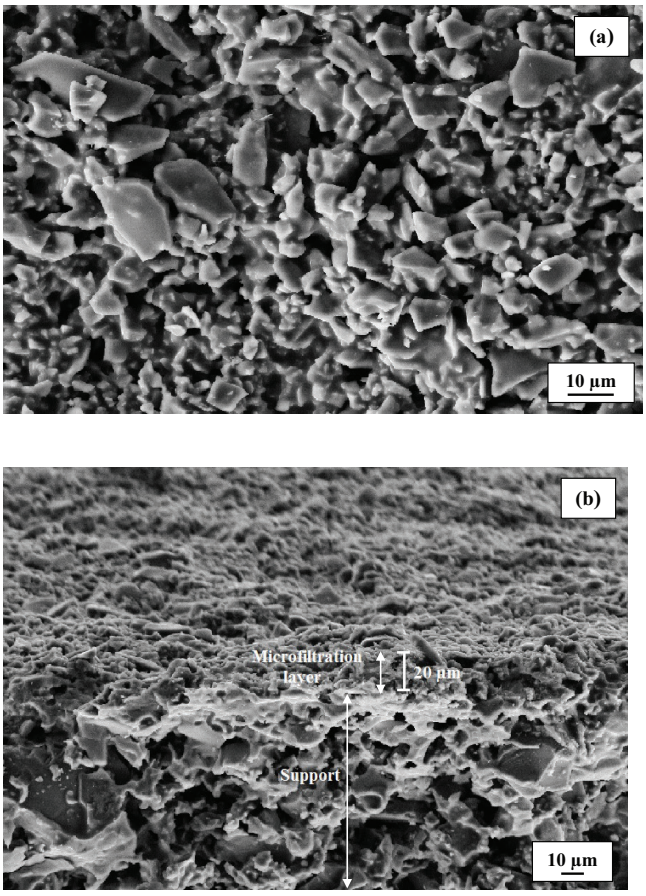

Fig. 9. SEM micrographs of the surface (a) and the cross section (b) of the microfiltration membrane sintered at 1,100°C.

3.4. Application to the treatment of the cuttlefish effluents

The study has been conducted with a cuttlefish wastewater sample supplied from cuttlefish conditioning and freezing process. Fig. 10 shows the permeate flux versus time of the sand microfiltration membrane sintered at 1100°C (T = 25°C, TMP = 1 bar). Permeate flux decreases in the first

15 min from 984 to 515 L/h m^2 then stabilizes at 464 L/h m^2 beyond 20 min. This behavior could be explained by the formation of concentration polarization and fouling due to the interaction between membrane material and solution [31]. The main characteristics of the raw and treated effluent are summarized in Table 3. It can be noticed that the chemical oxygen demand (COD) retention rate (COD achieved by a colorimetric method) has been about 97% and the turbidity of the treated effluent (Turbidimeter, Hach Ratio 2100A) has been very low (1.5 NTU). In term of quality, Fig. 11 shows a total elimination of suspended matter translated by a total discoloration of the raw effluent. These results confirm the high efficiency of this microfiltration membrane to cuttlefish effluent treatment.

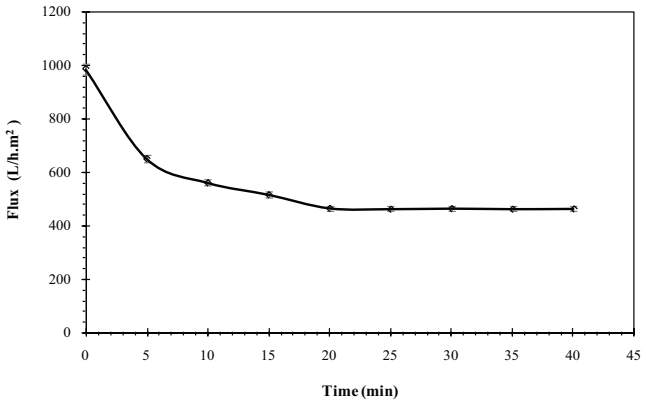

Fig. 10. Permeate flux vs. time of the sand microfiltration membrane sintered at 1,100°C (T = 25°C, TMP = 1 bar).

Table 3
Characteristics of the effluent before and after treatment

Sample	Raw effluent	Permeate (P = 1 bar)
pH	7.50	7.95
Conductivity (mS/cm)	3.900	0.966
Turbidity (NTU)	404.0	1.5
COD (mg/L)	5,625	145

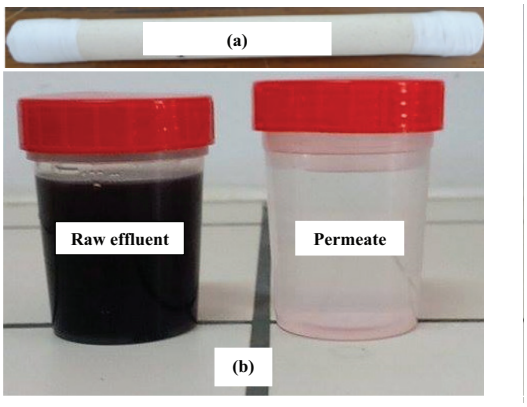

Fig. 11. Photographs of the microfiltration membrane sintered at 1,100°C (a) and the cuttlefish effluent before and after microfiltration treatment (b).

4. Conclusions

This study has reported the elaboration and the characterization of low-cost new ceramic microfiltration membrane based on Tunisian natural sand. The choice of the paste composition and the sintering conditions has favored the increase of the mechanical resistance while maintaining an important porous volume (porosity higher than 40%) and a good chemical resistance towards acid and basic solutions. Moreover, the elaborated supports remain advantageous since the used raw materials are very abundant in Tunisia. The active microfiltration layer obtained by slip casting process has displayed an excellent adhesion with the support, a high surface quality and a water permeability of 1,228 L/h m^2 bar. The application of the microfiltration membrane to the treatment of cuttlefish effluents has confirmed good performances in terms of COD and turbidity removal.

Acknowledgments

The authors would like to gratefully acknowledge Professors Gilles Regnier and Frederic Vales for advice about SEM analysis realized in the French laboratory "PIMM". This work was supported by Tunisian Ministry of Research.

References

[1] A. Barati, S. Khaleghi Rostamkolaei, H.R. Norouzi, S. Sharafoddinzadeh, Manufacture of tubular ceramic membrane supports using gelcasting, Adv. Appl. Ceram., 108 (2009) 203–210.
[2] Y.C. Woo, J.K. Lee, H.S. Kim, Fouling characteristics of microfiltration membranes by organic and inorganic matter and evaluation of flux recovery by chemical cleaning, Desal. Wat. Treat., 52 (2014) 6920–6929.
[3] W.J. Koros, R. Mahajan, Pushing the limits on possibilities for large scale gas separation: which strategies, J. Membr. Sci., 175 (2000) 181–191.
[4] A.F. Ismail, L.B. David, A review on the latest development of carbon membranes for gas separation, J. Membr. Sci., 193 (2001) 1–18.
[5] T.V. Gestel, C. Vandecasteele, A. Buekenhoudt, C. Dotremont, J. Luyten, R. Leysen, Alumina and titania multilayer membranes for nanofiltration: preparation, characterization and chemical stability, J. Membr. Sci., 207 (2002) 73–89.
[6] G.E. Romanos, T. Steriotis, A. Kikkinides, E.S. Kanellopoulos, N.K. Kasseelouri, Innovative methods for preparation and testing of Al_2O_3 supported silicalite-1 membranes, J. Eur. Ceram. Soc., 21 (2001) 119–126.
[7] S.H. Lee, K.C. Chung, M.C. Shin, J.I. Dong, H.S. Lee, K.H. Auh, Preparation of ceramic membrane and application to the cross-flow microfiltration of soluble waste oil, Mater. Lett., 52 (2002) 266–271.
[8] T. Tsuru, Inorganic porous membranes for liquid phase separation, Sep. Purif. Method., 30 (2001) 191–220.
[9] N. Saffaj, M. Persin, S. Alami Younssi, A. Albizane, M. Cretin, A. Larbot, Elaboration and characterization of micro-filtration and ultra-filtration membranes deposited on raw support prepared from natural Moroccan clay: application to filtration of solution containing dye sand salts, Appl. Clay Sci., 31 (2006) 110–119.
[10] H. Loukili, S. Alami Younssi, A. Albizane, J. Bennazha, M. Persin, A. Larbot, S. Tahiri, The rejection of anionic dyes solutions using an ultra-filtration ceramic membrane, Phys. Chem. News, 41 (2008) 98–101.
[11] S. Rakib, M. Sghyar, M. Rafiq, A. Larbot, New porous ceramics for tangential filtration, Sep. Purif. Technol., 25 (2001) 385–390.
[12] F. Bouzerara, A. Harabi, S. Achour, A. Larbot, Porous ceramic supports for membranes prepared from kaolin and doloma mixtures, J. Eur. Ceram. Soc., 26 (2006) 1663–1671.

[13] S. Sarkar, S. Bandyopadhyay, A. Larbot, S. Cerneaux, New clay–alumina porous capillary supports for filtration application, J. Membr. Sci., 392–393 (2012) 130–136.
[14] G. Chen, X. Ge, Y. Wang, W. Xing, Y. Guo, Design and preparation of high permeability porous mullite support for membranes by in-situ reaction, Ceram. Int., 41 (2015) 8282–8287.
[15] Y. Dong, X. Feng, D. Dong, S. Wang, J. Yang, J. Gao, X. Liu, G. Meng, Elaboration and chemical corrosion resistance of tubular macro-porous cordierite ceramic membrane supports, J. Membr. Sci., 304 (2007) 65–75.
[16] Ch. Liu, L. Liu, K. Tan, L. Zhang, K. Tang, X. Shi, Fabrication and characterization of porous cordierite ceramics prepared from ferrochromium slag, Ceram. Int., 42 (2016) 734–742.
[17] Y. Dong, S. Chen, X. Zhang, J. Yang, X. Liu, G. Meng, Fabrication and characterization of low cost tubular mineral-based ceramic membranes for micro-filtration from natural zeolite, J. Membr. Sci., 281 (2006) 592–599.
[18] A.I. Ivanets, T.A. Azarova, V.E. Agabekov, S.M. Azarov, C. Batsukh, D. Batsuren, V.G. Prozorovich, A.A. Ratko, Effect of phase composition of natural quartz raw material on characterization of microfiltration ceramic membranes, Ceram. Int., 42 (2016) 16571–16578.
[19] K. Suresh, G. Pugazhenthi, R. Uppaluri, Fly ash based ceramic microfiltration membranes for oil-water emulsion treatment: parametric optimization using response surface methodology, J. Water Process Eng., 13 (2016) 27–43.
[20] P. Belibi, M.M.G. Nguemtchouin, M. Rivallin, J.N. Nsami, J. Sieliechi, S. Cerneaux, M.B. Ngassoum, M. Cretin, Microfiltration ceramic membranes from local Cameroonian clay applicable to water treatment, Ceram. Int., 41 (2015) 2752–2759.
[21] N. Saffaj, M. Persin, S.A. Younsi, A. Albizane, M. Cretin, A. Larbot, Elaboration and characterization of microfiltration and ultrafiltration membranes deposited on raw support prepared from natural Moroccan clay: application to filtration of solution containing dyes and salts, Appl. Clay. Sci., 31 (2006) 110–119.
[22] S. Khemakhem, R. Ben Amar, R. Ben Hassen, A. Larbot, A. Ben Salah, L. Cot, Fabrication of mineral supports of membranes for microfiltration/ultrafiltration from tunisian clay, Ann. Chim. Sci. Mater., 31 (2006) 169–181.
[23] M. Khemakhem, S. Khemakhem, S. Ayedi, R. Ben Amar, Study of ceramic ultrafiltration membrane support based on phosphate industry subproduct: application for the cuttlefish conditioning effluents treatment, Ceram. Int., 37 (2011) 3617–3625.
[24] I. Jedidi, S. Khemakhem, A. Larbot, R. Ben Amar, Elaboration and characterization of fly ash based mineral supports for microfiltration and ultrafiltration membranes, Ceram. Int., 35 (2009) 2747–2753.
[25] S. Masmoudi, A. Larbot, H. El Feki, R. Ben Amar, Elaboration and characterization of apatite based mineral supports for microfiltration and ultrafiltration membranes, Ceram. Int., 33 (2007) 337–344.
[26] N. Tahri, I. Jedidi, S. Cerneaux, M. Cretin, R. Ben Amar, Development of an asymmetric carbon microfiltration membrane: application to the treatment of industrial textile waste water, Sep. Purif. Technol., 118 (2013) 179–187.
[27] S. Khemakhem, A. Larbot, R. Ben Amar, New ceramic microfiltration membranes from Tunisian natural materials: application for the cuttlefish effluents treatment, Ceram. Int., 35 (2009) 55–61.
[28] M. Khemakhem, S. Khemakhem, S. Ayedi, M. Cretin, R. Ben Amar, Development of an asymmetric ultrafiltration membrane based on phosphates industry sub-products, Ceram. Int., 41 (2015) 10343–10348.
[29] I. Jedidi, S. Saïdi, S. Khemakhem, A. Larbot, N. Elloumi-Ammar, A. Fourati, A. Charfi, A. Ben Salah, R. Ben Amar, Elaboration of new ceramic microfiltration membranes from mineral coal fly ash applied to waste water treatment, J. Hazard. Mater., 172 (2009) 152–158.
[30] S. Masmoudi, A. Larbot, H. El Feki, R. Ben Amar, Elaboration and properties of new ceramic microfiltration membranes from natural and synthesized apatite, Desalination, 190 (2006) 89–103.
[31] V. Chen, A.G. Fane, S. Maedani, I.G. Wenton, Particle deposition during membrane filtration of colloids: transition between concentration polarization and cake formation, J. Membr. Sci., 125 (1997) 109–122.